CONF-760111--1

PROMPT ALPHA AND REACTIVITY MEASUREMENTS ON FAST METAL ASSEMBLIES*

J. T. Mihalczo

Send correspondence to:
J. T. Mihalczo
Oak Ridge National Laboratory
P. O. Box X - Building 3500
Oak Ridge, TN 37830

OAK RIDGE NATIONAL LABORATORY
Oak Ridge, Tennessee 37830
operated by
UNION CARBIDE CORPORATION
for the
ENERGY RESEARCH AND DEVELOPMENT ADMINISTRATION

*Research sponsored by the Energy Research and Development Administration under contract with the Union Carbide Corporation.

DRAFT: JTM/dat
10/16/75
12/12/75

PROMPT ALPHA AND REACTIVITY MEASUREMENTS ON FAST METAL ASSEMBLIES

J. T. Mihalczo

INTRODUCTION

This paper summarizes and reviews the methods of reactivity determination and measurement of the prompt neutron decay, briefly describes the equipment requirements for such measurements for unmoderated and unreflected metal assemblies and presents experimental results to illustrate the methods. The primary reactivity determination methods used have been (1) stable reactor period measurements,[1] which are usually used near delayed criticality to calibrate the reactivity prior to burst initiation, (2) prompt reactor period measurements[2] which are useful to determine the reactivity early in the excursion, (3) inverse kinetics rod drop measurements[3] which obtain the reactivity as a function of time after a rod or reactor component is removed from the assembly, and (4) prompt neutron decay constant[4] measurements from which the reactivity can be obtained if corrections are made for changes in the neutron lifetime.[5] Inverse kinetics and decay constant measurements are usually used below delayed criticality although decay constant measurements have been performed above delayed critical.

The decay constant is usually obtained by the traditional pulsed neutron method[6] using a pulsed neutron source such as a Cockcroft-Walton accelerator or by the Rossi-α method.[7] The recent use of ^{252}Cf has resulted in some new techniques for determining the decay constant and reactivity which has some unique advantages over the traditional methods.[4,7,8-10] The theory[11] of these measurements is reviewed and some recent results are presented.

MEASUREMENT METHODS

The theory of the various measurement methods is presented and where possible particular experimental results are included to illustrate the method. The methods can be divided into two categories depending on whether the delayed neutrons play a significant role in the measurements or not. The prompt methods include the prompt period prompt neutron decay constant determination and other methods which use the correlation between the prompt neutrons emitted in fission chains. The delayed methods include the stable reactor period and inverse kinetics rod drop measurements. The newer method employing correlation with ^{252}Cf can be classified as a prompt method. It has been employed in measurements with fast metal assemblies but not as yet used for a fast burst reactor. It is a method that can determine the reactivity in the initial assembly far subcritical without the need for a calibration at delayed criticality.

REACTOR PERIOD MEASUREMENTS

The use of the inhour equation which is obtained from the point kinetics equation has traditionally been the primary means of calibrating the reactivity of fast pulsed reactors prior to pulsed operation. The inhour equation[1]

$$\rho(\$) = \frac{\ell}{\beta T_K} + \sum_i \frac{\beta_i/\beta}{1 + \lambda_i T_K} \qquad (1)$$

where

ℓ = prompt neutron lifetime

β_i = effective delayed neutron fraction for group i

β = total effective delayed neutron fraction

λ_i = decay constant for group i

This equation has six transient periods solutions, T_K and one stable reactor period. After a change in reactivity is made and the precursor concentrations have come to equilibrium, the stable reactor period is determined from the rate of change of the flux and it can easily be measured. The time to achieve a stable reactor period depends on the reactivity change and has been previously given.[12] Since the neutron lifetime is $\sim 10^{-8}$ sec for fast pulsed reactors near delayed criticality, the first term in the equation can be neglected. The measurement of T involves the determination of the slope of the exponential rise of the flux and is performed using counters and scaler-timers or ionization chambers and strip chart recorders.

Near prompt criticality $\lambda_i T_K \approx 0$ and the reactivity

$$\rho(\$) = \ell/\beta T + 1 \qquad (2)$$

Since the value of ℓ/β can be determined in prompt neutron decay constant measurements near delayed criticality, a measurement of the stable reactor period T early in an excursion

determines the reactivity that initiated the excursion. This reactor period is measured in the initial flux rise of prompt excursion before sufficient heat is produced to begin compensating for the reactivity insertion. It is usually obtained from the burst-shape detector by observing its output on a very sensitive range to obtain the period from the rate of exponential rise of the flux.

INVERSE KINETICS ROD DROP

The inverse kinetics rod drop methods is based on the use of the point kinetics equation to obtain the reactivity as a function of time from the neutron density as a function of time, t. For the case of negligible inherent neutron source, integration of the precursor concentration equation and substitution into the neutron density (n) equation yields after rearrangement. [13]

$$\rho(t) = \frac{\ell}{n}\frac{dn}{dt} + \beta - \frac{1}{n}\sum_i \lambda_i \beta_i \int_{-\infty}^{t} n(\xi) e^{-\lambda_i (t-\xi)} d\xi \qquad (3)$$

Again since $\ell \sim 10^{-8}$ the first term on the right can be neglected. This equation gives the reactivity as a function of time from a measurement of the neutron density up to time (t). In implementation of this method both digital and analog processing have been used.

Another example of the use of an analog computer was the determination of the reactivity for uranium metal cylinders.[14] The reactivity of the cylindrical assemblies was determined with the analog computer as follows. The BF_3 ionization chamber which provides the current input proportional to neutron density was placed coaxial with the uranium assembly (Fig. 1). The distance between the center of the chamber and the center of the assembly was 119 cm. Lead, 5 cm thick and 20 cm square, was placed in contact with the base of the chamber and between the chamber and the cylinder. All outer surfaces of the lead and of the chamber were covered with 0.1-cm-thick cadmium. An aluminum or a uranium cylinder, coaxial with the fixed uranium assembly, was remotely moved toward it until the system reached delayed criticality at a given power. This cylinder was then removed 25.4 cm in 0.3 sec followed by an additional displacement of 30.5 cm in 1.2 sec. From the neutron density as a function of time, the

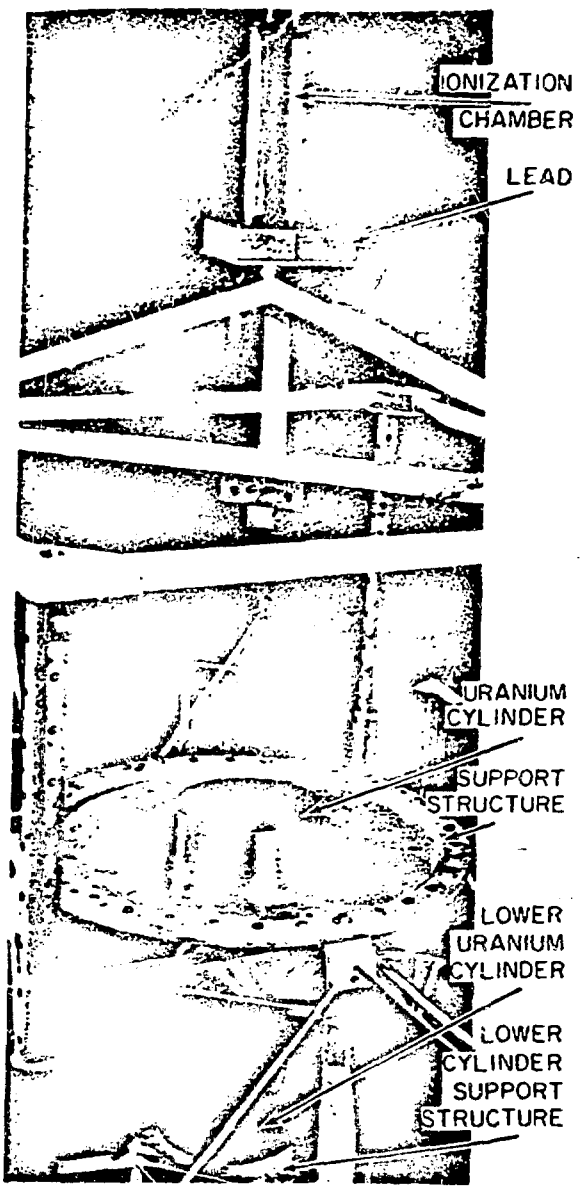

Fig. 1. Uranium cylinder and ionization chamber location for the analog computer measurements. The stationary cylinder whose reactivity is to be determined is on a stainless steel diaphragm and the lower cylinder, which upon raising brings the system to delayed criticality, is mounted on an aluminum support.

computer determined the reactivity and listed it in digital form every 0.5 sec. The reactivity after complete removal of the cylinder was interpreted as the reactivity of the fixed assembly assuming the results were not affected by the neutron decay in the movable cylinder displaced 56 cm. Figure 1 is a photograph of one of these systems after shutdown with the cables to the chamber and the cadmium removed. The reactivities of some of the cylinders measured by the analog computer are given in Table 1.

Typical results of analog measurements of control rod calibration for the Army Pulse Radiation Facility Reactor (APRFR) at Aberdeen, Maryland while it was undergoing initial tests at Oak Ridge[15] as shown in Fig. 2. In these measurements the reactor was adjusted to delayed criticality with the rod, for which the calibration was desired, inserted. The rod was then continuously withdrawn and from the reactivity as function of time and the rod positions as a function of time, the reactivity vs control rod position curve was obtained. This technique provided a rapid calibration of control rods since it does not depend on precursor concentration equilibrium. Some additional measurements of the safety block worth as a function of position were also obtained by this method and are given in Table 3.

Analog implementation of this method is presently being used in the safety system of Phenix in France.[16] Various digital implementation of this method have also been used.[17, 18]

Table 1. Comparison of Subcritical Reactivities of Uranium Cylinders Determined by Analog Computer and by Prompt Neutron Decay Constants

Cylinder Diameter (cm)	Cylinder Height (cm)	Subcritical Reactivity (dollars)[a]	
		From Computer[b]	From Prompt Neutron Decay Constant
38.090	7.502	2.77	3.14
38.091	7.337	4.95	5.29
38.090	7.016	9.28	9.24
38.091	6.693	13.55	13.94
38.090	6.373	18.29	18.94
38.089	6.055	22.93	23.37
38.090	5.734	28.42	28.57
38.090	5.419	33.86	33.58
27.929	8.431	2.04	2.00
27.937	8.266	3.85	3.71
27.933	8.097	5.38	5.36
27.933	7.943	7.33	7.30
27.935	7.641	11.01	11.07
27.935	7.332	15.06	14.92
27.935	7.005	19.95	18.82
27.934	6.678	24.56	23.57
27.933	6.356	28.82	27.65
17.771	10.184	13.63	13.48
17.771	9.234	22.57	20.29
17.771	8.281	32.88	28.40

a. Reactivity listed here is $(k - 1)/k\beta$.

b. The analog computer determines $(k - 1)/\beta$. A value of β of 0.00645 was used to make the conversion to $(k - 1)/k\beta$. The reactivities have been corrected for the assumption in analog computer than $\alpha = (k - 1 - \beta)/\ell$ rather than $\alpha = (k - 1 - k\beta)/\ell$. This correction is larger for the shorter cylinders but at most a 0.6% decrease in the reactivity.

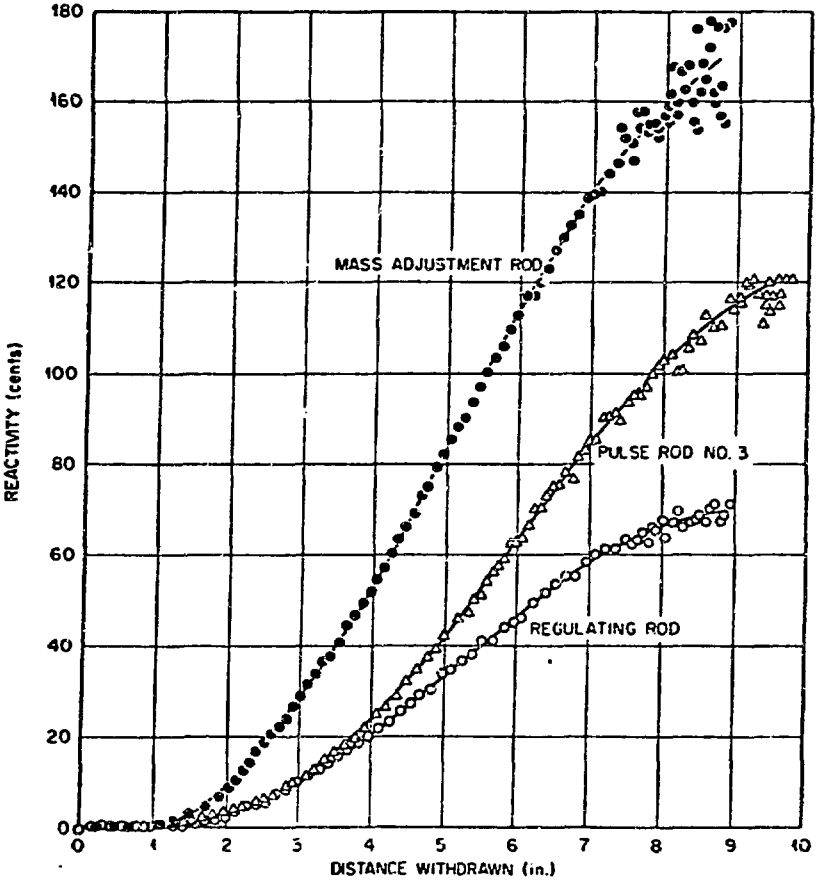

Fig. 2. The Reactivity of the Control Rods and Pulse Rod as a Function of Position in the Core.

Core Height: 7.760 in.
Safety Tube Attached.

PROMPT NEUTRON DECAY CONSTANT MEASUREMENTS

The prompt neutron decay constant, $\alpha = T^{-1}$ can be used to obtain the reactivity of a subcritical configuration if the prompt neutron decay constant at delayed criticality is known and a correction is made for the change in the neutron lifetime from delayed critical to the subcritical state of interest. Since the delayed neutron fraction $\beta = -\alpha_{DC}\ell_{DC'}$ where the subscript refers to values at delayed criticality, the reactivity can be expressed in terms of ratio of prompt neutron decay constants and lifetimes and is given by

$$\rho(\$) - 1 = \ell\alpha/\ell_{DC}\alpha_{DC} \qquad (4)$$

For fast metal assemblies the ratio of the neutron lifetime in the subcritical configuration to that for delayed critical was obtained using the DOT transport theory code[19] to obtain the forward and adjoint angular fluxes to compute the prompt neutron lifetime, $\ell = (\varphi_s^+, (1/v)\ \varphi_d)/(\varphi_s^+, \nu f_s\ \Sigma_f \varphi_d)$ where φ_s^+ and φ_c are the static adjoint and the dynamic angular forward fluxes, f_s is the energy distribution of neutrons from fission, and where the integrations are over all variables.[20]

The prompt neutron decay can be measured by a variety of techniques: the pulsed neutron method,[6] the Rossi-α method[7] and by cross correlating the events in a detector with those in a chamber containing ^{252}Cf which provides neutrons which initiate fission in the system.[11] Each of these measurement methods will be described and the results of measurements presented along with their interpretation.

Table 2. Comparison of prompt neutron decay constants of uranium cylinders measured by Rossi-α and pulsed neutron techniques

Outside Diameter (cm)	Average Height (cm)	Prompt Neutron Decay Constant[a] (μsec^{-1})		
		Rossi-α	Pulsed Neutron	Randomly Pulsed Neutron
38.090	7.016	10.9 ± 0.1	--	10.5 ± 0.1
38.090	6.373	20.7 ± 0.1	--	20.7 ± 0.2
38.089	6.055	25.5 ± 0.4	25.1 ± 0.2	--
38.091	5.099	40.7 ± 0.5	--	41.0 ± 0.6
27.929	8.431	3.2 ± 0.1	--	3.1 ± 0.1
27.933	8.097	6.7 ± 0.1	6.9 ± 0.1	--
27.933	7.943	9.0 ± 0.1	8.7 ± 0.1	--
27.935	7.641	12.9 ± 0.1	12.8 ± 0.1	--
27.935	7.322	16.9 ± 0.2	16.8 ± 0.1	--
27.935	7.005	20.9 ± 0.2	--	20.1 ± 0.1
27.934	6.678	25.8 ± 0.2	25.4 ± 0.2	--
27.933	6.350	30.0 ± 0.3	29.6 ± 0.2	--
27.934	5.726	40.9 ± 0.6	39.4 ± 0.4	40.7 ± 0.2
17.771	12.090	--	--	3.37 ± 0.01
17.771	11.772	--	--	5.00 ± 0.1
17.771	10.817	--	--	10.50 ± 0.1
17.771	10.184	15.4 ± 0.1	15.5 ± 0.1	--
17.771	9.234	22.5 ± 0.2	22.4 ± 0.1	21.6 ± 0.3
17.771	8.281	30.9 ± 0.3	29.9 ± 0.2	--
17.771	7.967	34.4 ± 0.3	--	--
17.771	7.642	37.0 ± 0.2	--	--
17.771	7.332	44.2 ± 0.2	--	--
17.771	7.007	44.2 ± 0.2	--	43.7 ± 0.3

[a]Errors indicated are one standard deviation from least-squares analysis of data.

Pulsed Neutron Method

The pulsed neutron method first described by Bengston[6] consists of introducing into the assembly a short burst of neutrons and observing the time decay of the neutron population. After some initial transients the neutron population at all energies and at all points in the reactor decays at the same rate. This fundamental mode decay is characterized by the prompt neutron decay constant. The measurement consists of placing a pulsed neutron source such as a Cockroft-Walton accelerator and a neutron detector in the assembly. The location of the source and the detector to suppress higher mode decay has been previously described.[21] Since the prompt neutron decay constant for fast pulsed reactors at delayed criticality is $\sim 10^6$ sec^{-1}, the width of the pulse from the source should be less than one microsecond. Typical fundamental mode decay periods for subcritical metal systems are in the nanosecond to microseconds range, so fast-electronics-instrumentation requirements are essentially the same as in fast-neutron time-of-flight experiments. Neutron pulse widths in the nanoseconds range give low pulse yields (required for time resolution in the neutron detector) and provide the necessary sharp pulse cut-off compared with the decay period being measured. Such short pulses can be produced by sweeping the ion beam from a Van de Graaff or Cockroft-Walton accelerator across a suitable defining slit. Despite the low neutron yield per pulse, good statistical accuracy can be obtained in reasonable "run" time by sweeping the ion beam at high (megacycle) repetition rates. The data is accumulated on time analysis equipment which is triggered each time a burst of neutrons is produced. The pulses from the detector are stored according to their time of arrival at the analyzer after the trigger pulse. Least squares analysis techniques are used to determine the fundamental mode decay constant. In this analysis successively smaller

segments of the data are examined to establish the time during which a single exponential decay persists.

The prompt-neutron decay constant for uranium metal cylinders was measured by this technique using a 150-kV Cockcroft-Walton accelerator which produced pulses of 14.2-MeV (d, T) neutrons having a width at half maximum of 30 nsec and a repetition rate of 0.9 Mc.[14] The accelerator-target assembly was located on the axis of the cylinder, at distances of 10 to 20 cm from the flat surface, and the 0.635-cm-thick plastic scintillator was 2.5 cm from the other flat surface as shown in Fig. 3. The time distribution of events of the detector with respect to the trigger associated with the accelerator pulse was measured. Time intervals between successive signals from the detector and the trigger as short as 5 nsec could be measured by a time-interval counter that used delay lines for interpolation of the basic 40-nsec period of a crystal oscillator. A PDP-4 digital computer processed the binary information from the time interval counter and the composite system served as the time analyzer. The trigger pulse from the detector started a count of the 5-nsec intervals, or of a preselected binary multiple of this interval, and the succeeding pulse from the detector stopped this count. The number of intervals counted was recorded in the computer memory. The prompt neutron decay constants obtained from some of the measurements with the uranium cylinders are given in Table 2. The reactivity was obtained using Eq. (4) and the results of these measurements agree well with the results of inverse kinetics rod drop measurements using an analog computer (Table 1) where both measurement methods were made.

Pulsed neutron measurements have been made with the APRFR reactor at Oak Ridge both at delayed criticality and for a variety of subcritical configurations. The target of the accelerator was located at the midplane of the core about 1 in. from the lateral surface and the detector, a small spiral ^{235}U fission chamber, was placed at the midplane in one of the control rod holes. The fundamental mode time decay as a function of safety block position is shown in Fig. 4. The reactivity for the various configurations

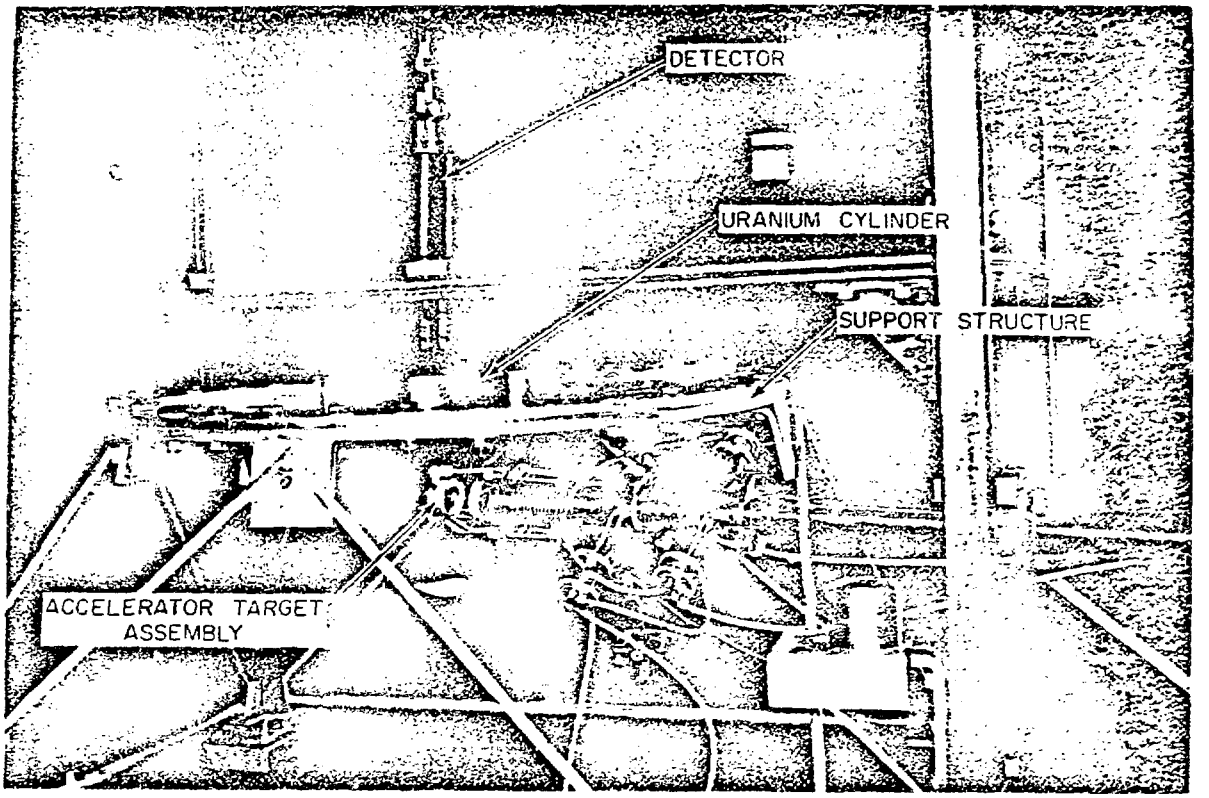

Fig. 3. Typical location of the detector and the accelerator-target assembly for the pulsed-neutron measurements.

ORNL-DWG 68-13697R

	DISTANCE THE SAFETY ANNULUS WAS WITHDRAWN[a] (in.)	PROMPT NEUTRON DECAY CONSTANT (μsec^{-1})	SHIFT IN[b] TIME SCALE (nsec)
●	11.50	11.87±0.18	-40
○	6.32	9.92±0.08	100
▲	5.00	7.97±0.04	120
△	4.00	6.14±0.06	180
▼	2.91	3.90±0.03	60
▽	2.03	2.56±0.02	200
●	1.62	2.01±0.02	100

a. DELAYED CRITICAL WITH THE SAFETY BLOCK INSERTED

b. THE TIME SCALE OF THE CURVES HAS BEEN SHIFTED TO DISPLAY THE DATA; THE TRUE TIME ZERO FOR EACH MEASUREMENT IS DISPLACED FROM THAT GIVEN ON THE ABSCISSA BY THE AMOUNT IN THIS COLUMN

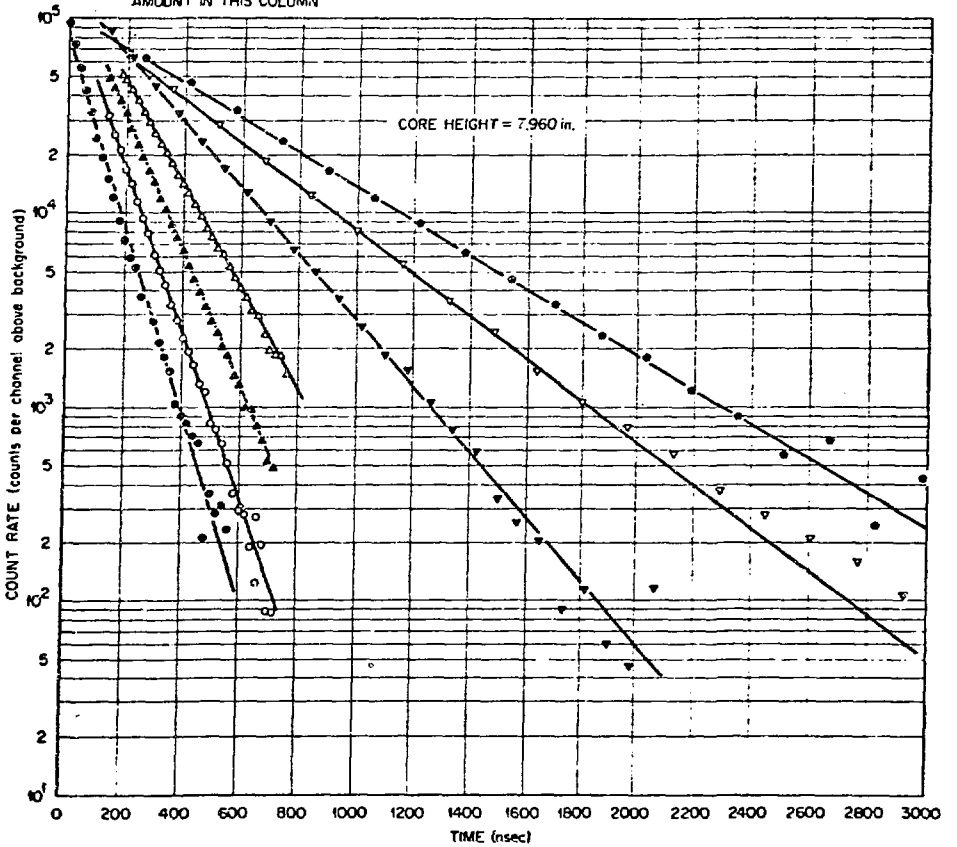

Fig. 4. Prompt Neutron Decay in the Reactor Determined by Pulsed Neutron Measurements. The decay in the damaged core was measured with the safety annulus at various positions.

of the APRFR are given in Table 3 where the results of inverse kinetics rod drop measurements are also presented. The agreement between reactivity determination by both methods is excellent.

Table 3. The Prompt Neutron Decay Constant in the Reactor Assembly for the Production of Pulses and the Associated Reactivity.

Core Height: 7.960 in.

Assembly Condition[a]	Prompt Neutron Decay Constant[b] (μsec^{-1})	Subcritical Reactivity (cents)	
		From Decay Constant[c]	From Analog Computer
Delayed criticality	0.675 ± 0.005	--	--
Regulating rod withdrawn	1.13 ± 0.01	67 ± 3[d]	69
Pulse rod No. 2 withdrawn	1.35 ± 0.03	100 ± 5[d]	104
Mass adjustment rod withdrawn	1.76 ± 0.02	161 ± 3[d]	172
Safety annulus withdrawn[e]			
1.62 in.	2.01 ± 0.02	207 ± 4	203
2.03 in.	2.56 ± 0.02	293 ± 5	295
2.91 in.	3.90 ± 0.03	509 ± 10	516
4.00 in.	6.14 ± 0.06	875 ± 17	--
5.00 in.	7.97 ± 0.04	1187 ± 16	--
6.32 in.	9.92 ± 0.08	1529 ± 25	--
11.50 in.	11.87 ± 0.18	1883 ± 45	--

a. A rod or the safety annulus was withdrawn from a delayed critical assembly as noted.

b. These values are averages where more than one measurement was made. The errors given are one standard deviation obtained from least-squares analyses of the data.

c. The uncertainty is that derived from the error in the prompt neutron decay constant.

d. The interpretation of the results of the decay constant measurements leading to these reactivities assumed that the prompt neutron lifetime did not change as the rod was withdrawn.

e. The prompt neutron lifetime for heights of 1.62 in, 2.03 in, 2.91 in, 4.00 in, and 6.32 in were 10.00 nsec, 10.06 nsec, 10.22 nsec, 10.40, nsec, and 10.75 nsec, respectively, and were obtained by interpolation of the calculated values for the safety blade inserted at 5.0 in, and at 11.50 in.

Rossi-α Measurements

In the point reactor model approximation the fundamental equation for calculating the time distribution function (the probability of a count in dt and another in dt_2) for an "ideal" Rossi-α experiment performed with two absorption detectors in a cross correlation experiment as given by[7]

$$F^2W_1W_2dt_1dt_2 + \frac{FW_2XRk^2}{2\alpha\ell^2}\, e^{-\alpha(t_2 - t_1)} \qquad (5)$$

where F is the fission rate and W_i is the detection efficiency for detector i in counts per reactor fission, X is the neutron dispersion number or Diven Factor $\overline{\nu(\nu - 1)}/\bar{\nu}^2$ where ν is the number of prompt neutrons per fission, and k is the prompt neutron multiplication factor. This equation also holds for auto correlation measurements with a single detector if the detection efficiencies in Eq. 5 are replaced with that of the single detector.

Three different types of time analyzers have been used for these measurements: (1) those that record all time intervals between counts in a second detector or the same detector that follow each input count from the first detector Type I, (2) those that accumulate time intervals between a trigger count and subsequent counts Type II, and (3) those that record counts only from adjacent pairs of counts Type III.[22] If the detection efficiencies are such that the probability of more than one count per analyzer trigger is small all three types of analyzer yield the same results. If not three different results may be obtained which have to be analyzed differently to obtain the correct reactor parameter.

The results of measurements with 17.77-cm-diam uranium metal cylinders are given in Fig. 5 and the prompt neutron decay constant obtained are listed in Table 14. For these measurements the neutron source of $\sim 10^7$ n/sec was placed in the center of the upper plane surface of the assembly and provided neutrons to initiate the fission chains. The

ORNL-DWG 67-9429

	CYLINDER HEIGHT (cm)	ORDINATE SCALE FACTOR[a]
●	10.184	0.8[b]
○	9.234	0.6
▲	8.281	2.0
△	7.642	8.0
♦	7.007	20.0

a. MULTIPLY PLOTTED POINT BY THE FACTOR TO GET DATA.

b. ABSCISSA SCALE FACTOR IS 1.5

ZERO OF TIME SET BY EVENT IN DETECTOR A.

BACKGROUND COUNTS SUBTRACTED.

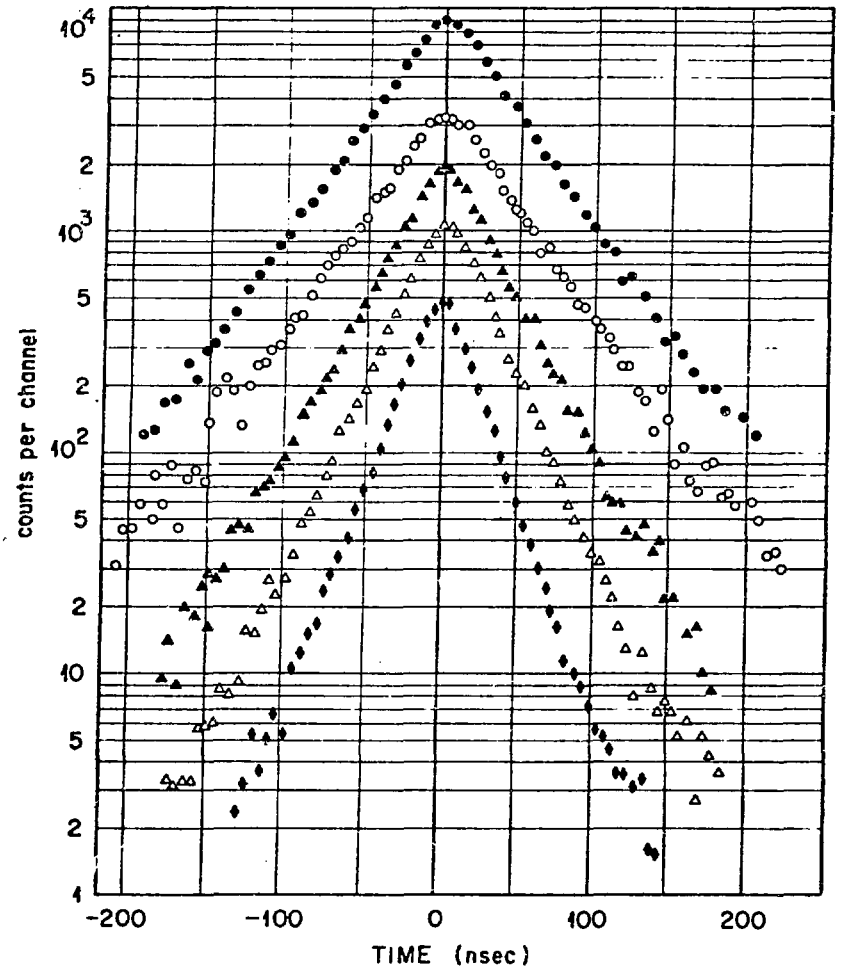

Fig. 5. Rossi-α Measurements for 17.77-cm-diam Uranium Cylinders.

detectors, proton-recoil-type plastic scintillators 5.1 cm in diam and 1.27 and 0.64 cm thich were located about 1.9 cm from the lateral surface. The pulses from the second detector were delayed with respect to those from the first detector so that the counts in the second detector that occurred before the event in the first detector were observed. The Type II analyzer, used for these measurements, was that described above for the pulsed neutron measurements.

The decay constants obtained by both the pulsed neutron and the Rossi-α methods are in excellent agreement (Table 2) and the reactivities obtained from prompt neutron decay measurements are an excellent agreement with those from inverse kinetics rod drop measurements.

Cross Correlation with ^{252}Cf

A special variation of a two detector cross correlation measurement has recently been described.[23, 24] This method has the simplicity of the Rossi-α cross correlation experiment but provides data much more efficiently. The ionization pulse produced by the fission products of fission in a chamber containing the spontaneously fissioning isotope ^{252}Cf establishes the time at which neutrons are injected into an assembly where they initiate fission chains. This starting pulse triggered a time analyzer and the response of the assembly was detected by a second detector whose pulses were sorted by the time analyzer. Thus, the prompt neutron decay is determined. The probability of a count in time interval dt after a californium fission is

$$F_c WF dt + \frac{\nu^{252}}{\nu} \frac{F_c W' k l_c}{S\ell l} e^{-\alpha t} dt \qquad (6)$$

where F_c is the ^{252}Cf spontaneous fission rate, W' is the detection efficiency in counts per californium fission, S is the number of reactor fissions per ^{252}Cf fission (note that $W'/S = W$ and $WF = W'F_c$), l_c is the importance of a neutron from ^{252}Cf fission and l is the average importance of neutrons from reactor fission. The point kinetics description of Eq. 6 assumes fundamental mode decay and no loss of triggers or counts by the detection systems and time analysis equipment. Since the correlated term in Eq. 6 contains the detection efficiency whereas the correlated term in Eq. 5 contains the square of the efficiency, the method correlating counts with ^{252}Cf fission will allow measurement of the decay constant in less time except in cases where the reactor fission rate F is much larger than F_c.

The ratio, A, of correlated counts in a randomly pulsed neutron measurement to those in a Rossi-α measurement is

$$A = \frac{2\nu_c i_c F_c \alpha \ell}{\nu X k_p W' I R F} = \frac{2\nu_c}{\nu R X W'} \frac{I_c}{I} \frac{1 - k_p}{k_p} \frac{F_c}{F} \quad . \qquad (7)$$

This ratio of correlated count rates, A, can be used to assess which method of measurement accumulates correlated information at a faster rate. As the multiplication factor or the detector efficiency approaches zero, the ratio becomes infinite; as the prompt-neutron multiplication factor approaches one, this ratio approaches zero. For a wide range of detection efficiency the Rossi-α method accumulates correlated counts faster near delayed criticality, while at far subcritical reactivities the reverse holds. The ratio is independent of the prompt-neutron lifetime, and for a given reactor it depends only on the prompt-neutron multiplication factor, the location of the ^{252}Cf source, the efficiency of the detector, and the ratio of the fission rate in the randomly pulsed neutron measurements to that in the Rossi-α measurements. If the Rossi-α measurements can be performed at high fission rates, i.e., $F \gg F_c$, or with high detection efficiency, then they may be more practicable. Large values of F may arise from the initiation of fission chains by a large number of delayed neutrons in assemblies at or above delayed criticality or by large inherent neutron sources such as those present in systems containing a large amount of ^{240}Pu.

This correlation method, which can be considered a randomly pulsed neutron method, enables the measurement of the prompt-neutron decay without the use of a complex pulsed neutron source where Rossi-α measurements are not practicable. Since in this technique the time behavior of the fission chains from initiation by neutrons from californium fission is observed, the measured decay contains more of the initial transient after introduction of the source neutrons than the Rossi-α method in which the decay is observed after the first detection of a particle from the fission chain.

To compare this technique with other decay constant methods, experiments were performed with the unmoderated uranium metal cylinders were previously studied by both the Rossi-α and the pulsed neutron methods. The plastic scintillator described above was used in these measurements. The time analyzer was a Type II analyzer which had a minimum channel width of 10 nsec and counts could be accumulated at a 10-MHz rate in channel in each sweep or a Type III analyzer consisting of a time to pulse height converter with a pulse height analyzer. Typical prompt neutron decays for these cylinders are shown in Fig. 6. Fig. 7 compares the decay obtained in both a randomly pulsed neutron with ^{252}Cf and in Rossi-α measurements with the same fission rate in the assembly for both types of measurements. The decay constants obtained in these measurements are given in Table 2.

Experiments have also been performed satisfactorily for plutonium system[25] with as much as 20 wt % ^{240}Pu and with moderated metal assemblies with decay constants as small as 3000 sec^{-1} where Rossi-α measurements are not practicable. Measurements with the Jezebal assembly[25] determined the reactivity as a function of the separation of the lower section to be 12.4, 28.1, 36.1, 40.9, and 46.7 dollars subcritical for separations of 0.32, 0.66, 1.27, 4.6, and 14,6 cm, respectively.

In determining the reactivity for this measurement by the methods of Sjostrand,[26] Gozani,[27] or Garelis-Russell[28] the contribution to the background due to the random nature of the source should be subtracted before analysis.

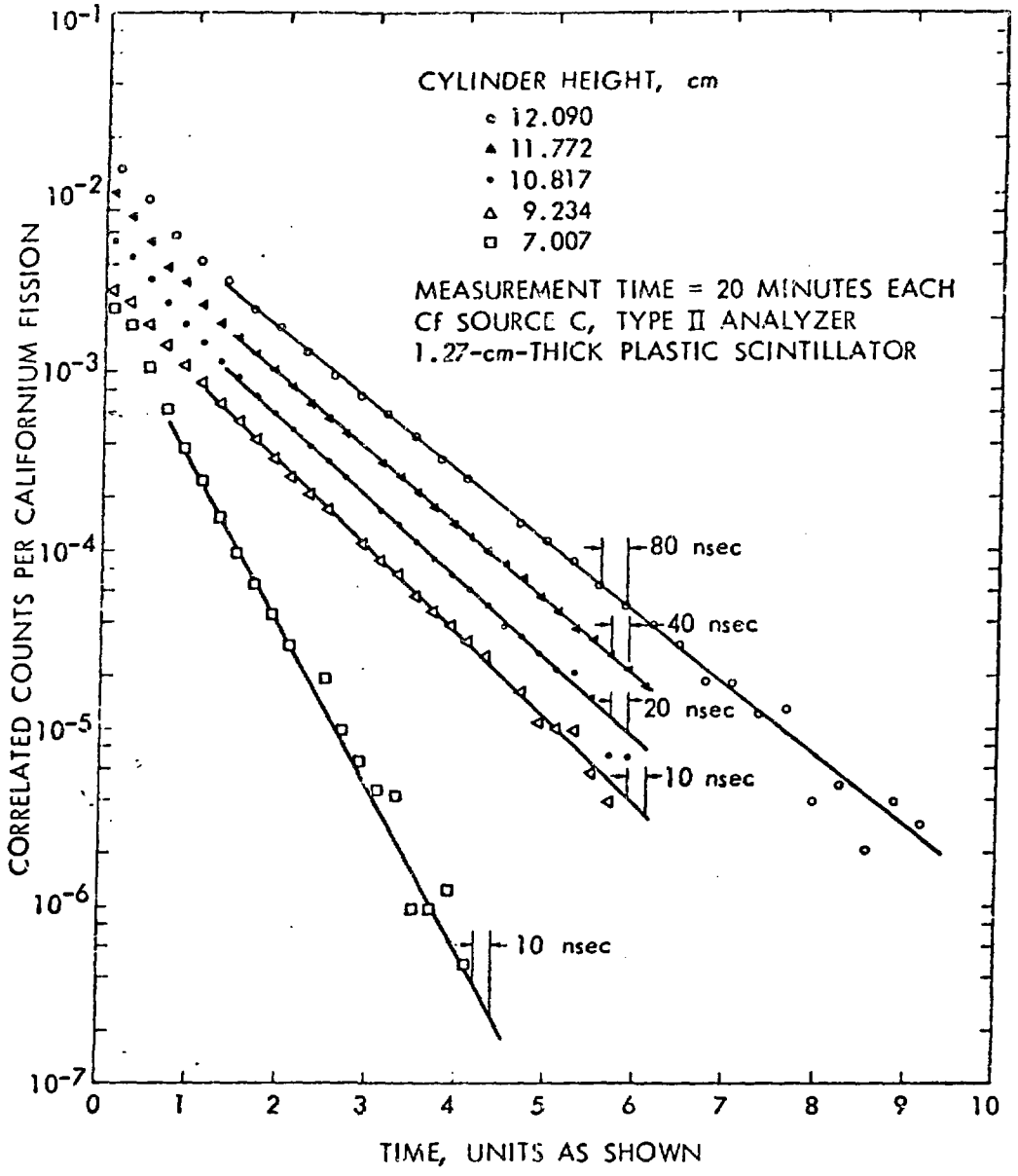

Figure 6. The prompt neutron decay in randomly pulsed neutron measurements for the 17.771-cm-diam unmoderated uranium cylinders.

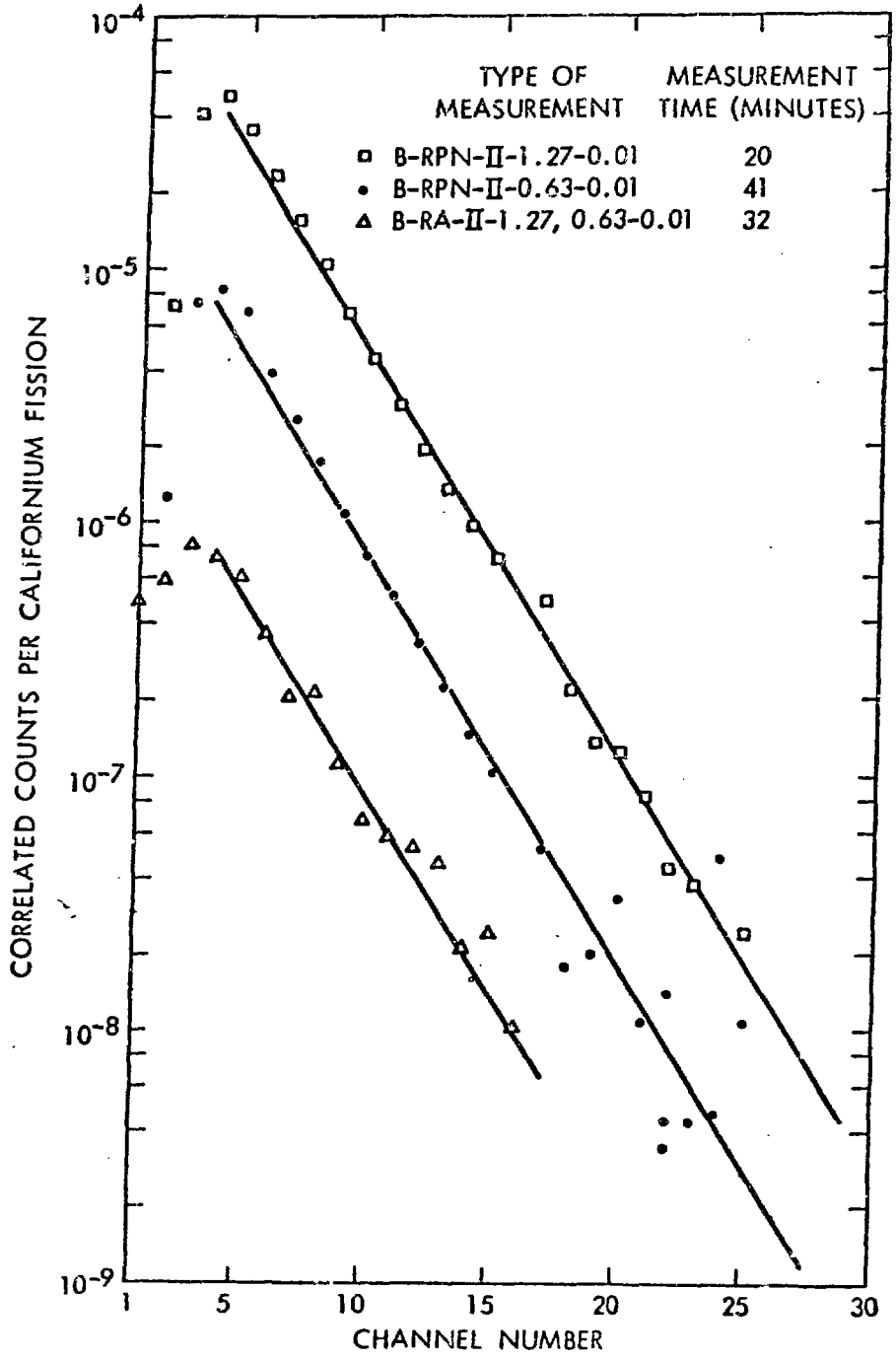

Figure 7. The comparison of the prompt neutron decay from randomly pulsed neutron measurements with that from a Rossi-α measurement for a 27.934-cm-diam, 5.726-cm-high uranium cylinder.

Reactivity Determination From Simultaneous Rossi-α and Randomly Pulsed Neutron Measurements

Consider the ratio AW' which is the ratio of the correlated counts per californium fission from the randomly pulsed neutron measurement to the correlated counts per detector count in the Rossi-α. The following expression,[24]

$$AW' = \frac{2\bar{\nu}_c I_c}{\bar{\nu} R X I}\left(\frac{1 - k_p}{k_p}\right), \tag{8}$$

can be used to determine the prompt reactivity in k units rather than in dollars and to compare calculated multiplication factor directly with a measured value. The use of Eq. (8) to obtain a reactivity does not depend on determination of properties of the reactor at delayed criticality nor does it require a calibration by other reactivity determination methods. Thus, it could be particularly useful in the initial startup of a reactor when the properties of the reactor at delayed critical are not known or a calibration near delayed critical cannot be made. It could also be useful as a reactivity determination method in experiments particularly where sufficient material to achieve delayed criticality is not available.

For a delayed critical system $k = 1 - \beta_{eff}$, where β_{eff} is the increment of the multiplication factor between delayed and prompt criticality. Thus, for a delayed critical system, the product $A_{DC}W'$ is

$$A_{DC}W' = \frac{2\,\nu^{252} I_c}{\bar{\nu} R X I}\,\frac{\beta_{eff}}{1 - \beta_{eff}}\,. \tag{9}$$

The values of AW' from measurements with a uranium metal sphere were obtained for three different ^{252}Cf chamber designs with spontaneous fission rates varying from 2.6 to 9 x 10^4 fissions/sec, for a variety of ^{252}Cf chamber and spiral fission counter locations and for various reactivities (Table 4). Typical prompt neutron decay from both Rossi-α and randomly pulsed neutron measurements are given in Fig. 8. In measurements with the annular ^{252}Cf chamber at delayed criticality, the values of AW' for spiral fission counter location at radii of 0, 3.81 and 4.27 cm were within 2.3% of each other, thus verifying that the measurements were independent of spiral fission counter location. These results also verified that the number of events in the spiral fission counter from neutrons coming directly from the ^{252}Cf source were negligible compared to neutrons from fission chains in the assembly since the distance between the ^{252}Cf chamber and the spiral fission counter was varied. The measurements of AW' performed in 1975 gave results that were within 0.1% of those of 1972.

The average value of the effective delayed neutron fraction obtained from these measurements was (60.6 ± 0.2) x 10^{-4}, and the results of the various measurements are in excellent agreement. The total spread in the measured values is 8.4% with the value of the effective delayed neutron fraction varying between 58.6 x 10^{-4} and 63.5 x 10^{-4}. The variation in the values with reactivity was determined in two sets of measurements; 4.6% for reactivities of 0, +29, and +52 cents with a 1.27-cm-diam parallel plate ^{252}Cf chamber near the sphere center; and 1% for reactivities of 0 and -21 cents with a annular ^{252}Cf chamber near the surface of the sphere; thus, confirming the dependence on reactivity. Measurements were performed with the location of the ^{252}Cf chamber and the spiral fission counter essentially interchanged (1.27-cm-diam parallel plate chamber at radii of 0.26 and 6.27 cm and the spiral fission counter at radii of 6.84 and 0 cm) and the delayed

Table 4. Measured values of WA for a variety of source detector configurations

Californium Chamber[a]			Spiral Fission Counter[b]				
Number	Location	Radius (cm)	Location	Radius (cm)	Reactivity[c] (cents)	WA x 10^{-4} [d]	Effective Delayed Neutron Fraction
59	Diametral Hole	6.90	Diametral Hole	4.27	0	144.8 ± 0.6	58.8 ± 0.6
59	Diametral Hole	6.90	Diametral Hole	0	-21	113.5 ± 10.6	58.6 ± 2.2
59	Diametral Hole	6.90	Diametral Hole	0	0	145.2 ± 0.5	59.2 ± 0.2
59	Diametral Hole	6.90	Diametral Hole	3.81	0	148.2 ± 0.6	60.2 ± 0.3
2	Surface	8.92	Diametral Hole	0	0	57.0 ± 0.3	60.8 ± 0.2
61	Diametral Hole	0.26	Surface Hole	6.84	0	313.0 ± 2.0	60.7 ± 0.4
61	Diametral Hole	0.26	Surface Hole	6.84	0	312.6 ± 3.1[e]	60.7 ± 0.6
61	Diametral Hole	0.26	Surface Hole	6.84	+29	233.2 ± 3.2[e]	63.5 ± 0.8
61	Diametral Hole	0.26	Surface Hole	6.84	+52	151.7 ± 2.2[e]	62.5 ± 0.9
61	Surface Hole	6.277	Diametral Hole	0	0	261.3 ± 1.9	61.4 ± 0.3
61	Surface Hole	6.277	Diametral Hole	4.27	0	167.4 ± 0.9	62.1 ± 0.5

[a]Counter 61 had a 1.27-cm-diam and could be located in the diametral hole or the surface hole and counter 59 had a 0.953-cm-diam and could be placed near the surface only.

[b]The 1.27-cm-diam spiral fission counter could be placed at any radius in the diametral hole or in the surface hole.

[c]Deviations from the approximate reactivity given in this column were acounted for in the determination of the effective delayed neutron fraction.

[d]The number of pairs of Rossi-α and randomly pulsed neutron measurements that were used to obtain this average were 83, 8, 130, 7, 79, 71, 30, 17, 20, 82 and 34, respectively. Error given is the standard deviation of the mean.

[e]Measurements performed in 1975; all other measurements listed were performed in 1972.

neutron fraction determined differed by 1.2%. This interchange of detector locations and the agreement of the measurements for the three different ^{252}Cf chambers verified that the neutron importance values used for the ^{252}Cf chambers were correct.

The effective delayed neutron fraction determined in these measurements is somewhat lower (11%) than that obtained from measurements of the central worth of uranium in this sphere (0.0066) and the calculated value (0.0066) which agrees with previous measurements at Los Alamos Scientific Laboratory (0.0066 from Ref. 23). It also is lower (6%) than the delayed neutron fraction obtained for fast fission of the ^{235}U isotope.[31,32,33] The validity of the assumption of point kinetics in the interpretation of these measurements is questionable although the independence of the results on location of the detectors and source seems to verify the assumption of point kinetics. This low value of the effective delayed neutron fraction may result from the improper correction of point kinetics for spatial effects. This factor has been obtained from previously measured fission density and neutron importance distributions and could not significantly be in error due to the functions used to obtain it since these were previously measured but this factor maybe in error theoretically. Values of this correction factor are as much as 30% larger for a bare uranium sphere have been proposed by others.[34] If this spatial correction to point kinetics were 11% larger this effective delayed neutron fraction determination would be in agreement with other measurements.

REACTIVITY DETERMINATION FROM POWER SPECTRAL DENSITY MEASUREMENT WITH ^{252}CF

Frequency domain analysis of correlated signals provide some useful relationships which can be used to obtain the reactivity. The use of Eq. (8) requires larger and larger ^{252}Cf sources the further subcritical the measurement. The limitation of pulse counting methods require that measurements utilizing this method requiring sources of > 15μg of ^{252}Cf be performed by frequency domain analysis. The auto-and cross-power spectral densities have previously been derived for the frequency domain measurements (Ref. 11). For a reactor with three detectors, one of which is the ^{252}Cf ionization chamber (detector 1) which provides the initiators of fission chains and two detectors (2 and 3) which detect neutrons from the fission chains, the auto- and cross-spectral densities are

$$G_{11} = |h_1(\omega)|^2 F_c\left(31\overline{q_\alpha^2} + \overline{q_c^2}\right), \tag{9}$$

$$G_{22} = |h_2(\omega)|^2 \left[FW_2\overline{q_2^2} + \frac{W_2^{2-2}}{\bar{\nu}^2}\,|H_s(\omega)|^2 G_s\right], \tag{10}$$

$$G_{23} = h_2^*(\omega)h_3(\omega)\,\frac{W_2W_3\overline{q_2}\;\overline{q_3}}{\bar{\nu}^2}\,|H_s(\omega)|^2 G_s, \tag{11}$$

$$G_{12} = \overline{q_c}h_1^*(\omega)h_2(\omega)\,\frac{W_2\overline{q_2}}{\bar{\nu}}\,H_s(\omega)G_c', \tag{12}$$

where $h_i(\omega)$ = frequency, ω, response of detection system i

q = charge released per interaction in a detector or the ^{252}Cf chamber. Subscript α refers to alpha decay and subscript c to spontaneous fission of ^{252}Cf.

$\bar{\nu}_i$ = average number of neutrons per inherent source fissions

$H_s(\omega)$ = source transfer function of the reactor

Now, the source spectral density, G_s, is

$$G_s = \bar{\nu}^2 XFR\left[1 + \frac{V}{XR} + \frac{F_i I_i}{FI}\,\frac{\overline{\nu_i^2}}{XR\bar{\nu}^2} + \frac{F_c}{F}\,\frac{I_c}{I}\,\frac{\overline{\nu_c^2}}{XR\bar{\nu}^2}\right] = \bar{\nu}^2 X'FR, \quad (13)$$

where X' is a modified form of the neutron dispersion number, I_i is the neutron importance for inherent source fission, and V equals $(2\beta - \rho)/[(1 - \beta)\bar{\nu}]$. There are expressions similar to Eqs. (10) and (12) for G_{33} and G_{23}.

The methods for determination of the reactivity from the power spectral densities given by Eqs. (9) to (12) can be classified into three categories: (1) the existing methods related to the conventional two-detector auto- and cross-power spectral densities, G_{22}, G_{33}, and G_{23}; (2) those that determine parameters which have been used previously for reactivity determinations from the cross-power spectral densities with Cf, G_{12}; and (3) new methods that determine the reactivity without a calibration near delayed criticality.

The use of previously described methods, such as the determination of the reactivity from the breakfrequency of APSDs and CPSDs or from the coherence amplitude, γ_{23}, requires a knowledge of the breakfrequency and coherence amplitude at some reference state, usually near delayed criticality, for which the reactivity is known, as well as the change in the prompt-neutron generation time or detection efficiency between the reference state and the reactivity state of interest. These breakfrequency noise analysis methods require corrections for the frequency response functions of the detection system, $h_2(\omega)$ and $h_3(\omega)$, which are usually obtained from measurements in which the detection system is exposed to the

random emission of a neutron source [this input is a white noise source, and thus, the measured frequency response will be $h_i(\omega)$].

The measurement of the cross power spectral density with ^{252}Cf allows the determination of the breakfrequency from which the prompt neutron decay constant can be obtained. After a correction is made for the frequency response of the detection systems, the CPSD, G_{12}, is proportional to the source transfer function of the reactor, $[(\alpha + i\omega)\Lambda]^{-1}$, and $|G_{12}|^2$ can be fitted by a least-squares method to determine the value of α. This measurement also allows the determination of the prompt neutron decay constant in a novel way, since the source transfer function can be written as $(\alpha - i\omega)/\alpha^2 + \omega^2)\Lambda$, and thus G_{12} has a real and an imaginary part which can be obtained by present digital Fourier analyzers. Since the values of ω are known, the product of the ratio of the real to the imaginary part of G_{12} and the frequency ω is constant and equal to the prompt-neutron decay constant. The subcritical reactivity can be obtained in the usual way from the ratio of this decay constant to that for delayed bration state after it has been corrected for the change in the neutron lifetime from the calibration state to the subcritical state of interest. The constancy of this ratio can be used to validate the point kinetics model since the presence of higher modes would cause the value of α determined in this way to be a function of frequency. The constancy of the ratio would also verify whether the correction for the frequency response of the instrumentation is correct.

Various combinations of spectral densities were examined in order to determine if any additional information could be obtained from the simultaneous measurement of all four spectral densities represented by Eqs. (9), (11), and (12). To develop a method for measuring the reactivity, consider the following combination of spectral densities:

$$\frac{G_{12}^{*}G_{13}}{G_{11}G_{23}} = \frac{\gamma_{12}\gamma_{13}}{\gamma_{23}} = \frac{1}{B_c(1 + C_\alpha)}\left(\frac{\bar{\nu}_c I_c}{\bar{\nu} I}\right)^2 \frac{1}{RX'}\frac{F_c}{F} . \qquad (14)$$

where γ are the coherence values between the various pairs of detectors and B_c is the ratio $\overline{q_c^2}/\bar{q}_c^2$ and C_α is the ratio $3\overline{q_\alpha^2}/\overline{q_c^2}$ where q_c and q_α are the ionization produced in the californium chamber from spontaneous fission and alpha particle decay, respectively.

The ratio of spectral densities given in Eq. (14) is independent of frequency. Thus, the constancy of Eq. (14) as a function of frequency could be used to validate the model as well as to determine whether the experimental data from the noise analysis measurement have adequate precision. Since $FI\bar{\nu} = (F_c I_c \bar{\nu}_c + F_i I_i \bar{\nu}_i)\frac{k}{1-k}$, Eq. (14) can be rearranged to yield the subcritical reactivity ρ in Δk units, where k is the neutron multiplication factor including the effect of delayed neutrons. Thus,

$$\frac{1-k}{k} = \frac{G_{12}^{*}G_{13}}{G_{11}G_{23}} \frac{(F_c I_c \bar{\nu}_c + F_i I_i \bar{\nu}_i)}{(F_c I_c \bar{\nu}_c)} \frac{I\bar{\nu}}{I_c \bar{\nu}_c} B_c(+ C_\alpha)X'R . \qquad (15)$$

No correction for the frequency response of the instrumentation is required, because the transfer functions for the detection system electronics are canceled in forming the ratio given by Eq. Since X' defined by Eq. (13) contains the reactivity and differs from X far subcritical, Eq. (15) should not be used for far subcritical reactivities. Substitution for X' and rearrangement gives the following expression for the reactivity

$$\frac{1-k}{k} = \frac{G_{12}^{*}G_{13}}{G_{11}G_{23}} \left[\frac{P[1 + 2\beta/XR(1 - \beta)\bar{\nu}]}{1 - \frac{G_{12}^{*}G_{13}}{G_{11}G_{23}}\frac{P}{\bar{\nu}}\left[P_2 + \frac{1}{XR(1-\beta)}\right]}\right] \qquad (16)$$

where

$$P = \frac{I\bar{\nu}}{I_c\bar{\nu}_c} B_c(1 + C_\alpha) RXY \qquad (17)$$

$$Y = \frac{F_c I_c \bar{\nu}_c + F_i I_i \bar{\nu}_i}{F_c I_c \bar{\nu}_c} \qquad (18)$$

$$P_2 = \left[\frac{\overline{\nu_i^2}}{\overline{\nu_i}} (Y - 1) + \frac{\overline{\nu_c^2}}{\overline{\nu_c}} \right] \Big/ XRY \qquad (19)$$

Eq. (15) or (16) do not depend on detection efficiency, but do depend on the properties of the detection system for ^{252}Cf fission which can be determined outside the reactor. The ratio of the effective neutron production rates, Y, can be determined from the change in count rate when the ^{252}Cf source is inserted into the subcritical reactor. The values of R and X can be determined from calculation and other measurements and are insensitive to large changes in reactivity. The values of the numbers of neutrons per fission are known and the relative importance l/l_c can be calculated or obtained from other measurements. Thus, solution of Eq. (15) or (16) gives the reactivity or neutron multiplication factor in k units. This method requires neither a calibration near delayed criticality ncr corrections for neutron lifetime or detection efficiency changes, which other noise analysis methods do require.

For a pulse mode electronics system and a ^{252}Cf chamber in which all the alpha pulses can be discriminated, $C_\alpha = 0$ and $B_c = 1$ and Eq. (14) reduced to $\left(\frac{\bar{\nu}_c l_c}{\bar{\nu} l} \right)^2 \frac{1}{RX^\tau} \frac{F_c}{F}$. Thus, for pulse mode operation of the californium ionization chamber the reactivity does not depend on the properties of the californium fission detection system.

For pulse mode operation of the ^{252}Cf chamber, it has been shown (Ref.) that the ratio of spectral densities $R_e(G_{12})/|G_{23}|$ when both spectral densities have been corrected for the frequency response of the instrumentation reduces to the time domain expression given by Eq. (8).

Spectral Density Measurements with a Uranium Metal Sphere and Cylinders

Experiments with the bare uranium (93.2 wt % ^{235}U) metal which has previously been studied in a series of time domain measurements using ^{252}Cf were performed to verify the theory of this ^{252}Cf noise analysis measurement. This sphere had the following advantages for this type of measurement: (1) the properties of the sphere required for the interpretation of this measurement have previously been measured in connection with time domain measurements, (2) geometrical simplicity and single homogeneous material, (3) negligible inherent source, and (4) ^{6}Li glass scintillators adjacent to the surface would have a high detection efficiency ($\sim$ 0.1 events/assembly fission) because it is a small high leakage system and the scintillators are sensitive to gamma rays as well as neutrons. Items (1) and (2) simplified the interpretation of the results; item (3) allowed the use of existing chambers containing ^{252}Cf which were used in the time domain measurements; item (4) permitted the measurements to be performed in a short time, < one minute of data sampling. One of the disadvantages of uranium metal assemblies for this type of measurement was that an independent determination of the reactivity from breakfrequency noise analysis was not possible because the lowest breakfrequency from noise analysis for these systems in their most reactive condition is about 160 kHz, essentially beyond the capability of the Fourier analyzer used for the measurements.

It was desirable to perform measurements with small uranium metal assemblies at lower reactivities to verify the theory of this type of measurement. To reduce the reactivity further by the removal of the top section of the sphere assembly would have resulted in a complicated three-dimensional system for which it would be difficult to calculate the quantities required to interpret this type of measurement. Unreflected and unmoderated uranium cylinders which had previously been assembled and the reactivity calibrated as a

function of height by both the pulse neutron and inverse kinetics rod drop technique down to about 30 dollars subcritical were used to test this spectral density method. Since the calculated and measured fission density and neutron importance distribution for the bare sphere agreed very well with measurements, transport theory calculations should be adequate for these two-dimensional assemblies of the same material. Since the parallel plate ionization chamber used to the cylinder exponents was cylindrically symmetric and located on the axis, it could be mocked up precisely for the calculation of the neutron importance of neutrons from spontaneous fission of ^{252}Cf in the counter.

Power Spectral Densities

Typical power spectral densities for the sphere with a reactivity of 29 cents subcritical are shown in Fig. 9 where an auto power spectral density (G_{33}) of one of the ^{6}Li glass scintillators, the cross power spectral density (G_{23}) between the two glass scintillators, and the square of the cross power spectral density ($|G_{13}|^2$) between one of the scintillators and the ^{252}Cf chamber are plotted as a function of frequency up to 100 kHz. Since these spectral densities have been corrected for the frequency response of the instrumentation, the rolloff at high frequency is associated with the breakfrequency or decay constant of the sphere at this reactivity. The breakfrequencies determined in the least square fitting of the cross power spectral densities were 165, 157, and 163 kHz (associated errors are large due to frequency limitations of Fourier analyzer) are close to the expected breakfrequency for this assembly. The real and imaginary parts of the cross power spectral density with ^{252}Cf are plotted as a function of frequency in Fig. 10. The near-zero values of the imaginary part at low frequency, which is proportional to $\omega/\alpha^2 + \omega^2$, results from the value of the prompt neutron decay constant $\alpha > 10^6$ sec^{-1}.

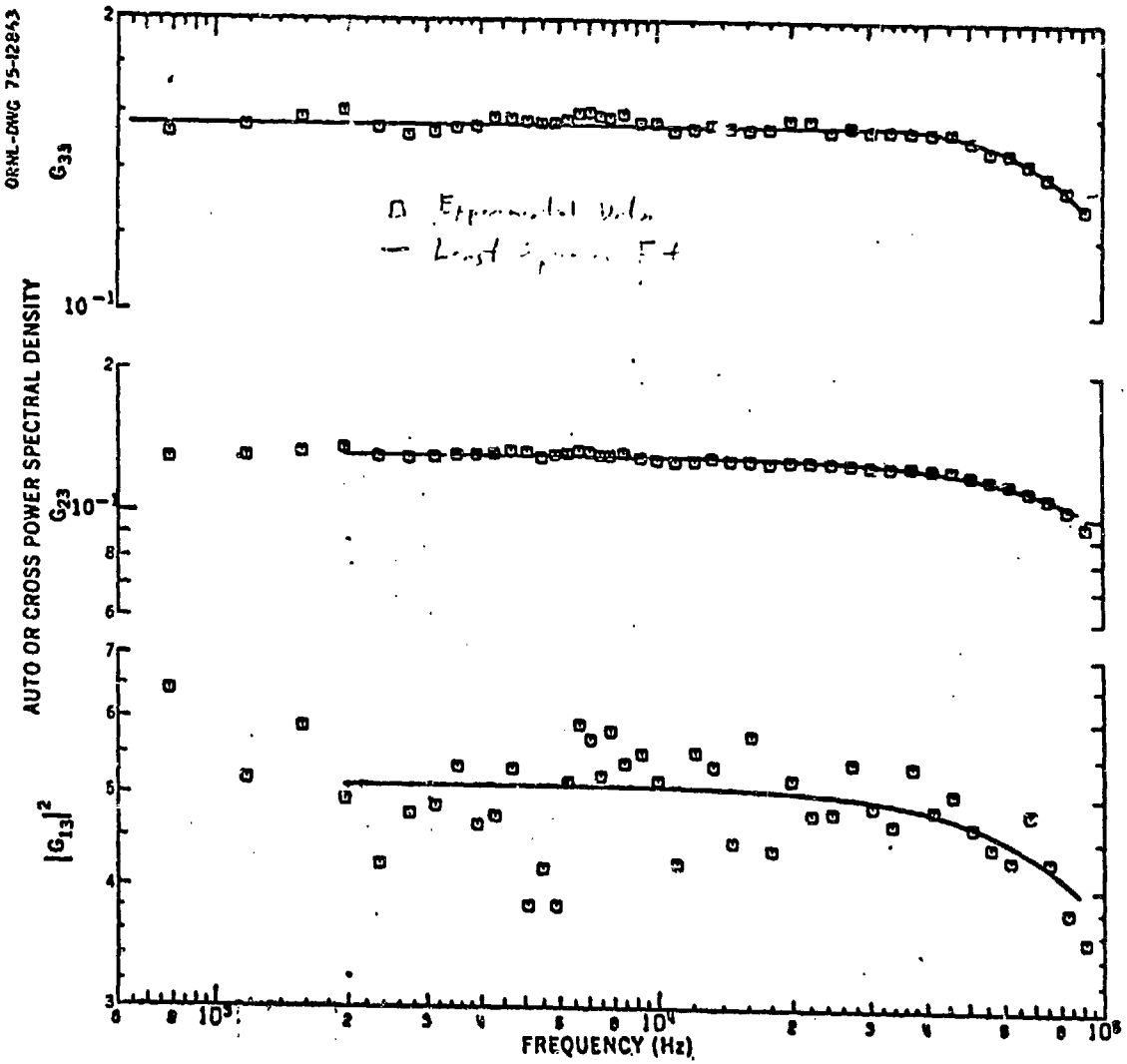

G_{c33}

G_{c23}

$|G_{c13}|^2$

37

Fig 18 Power Spectral Densities, G_{33}, G_{23}, $|G_{13}|^2$ For the uranium sphere with

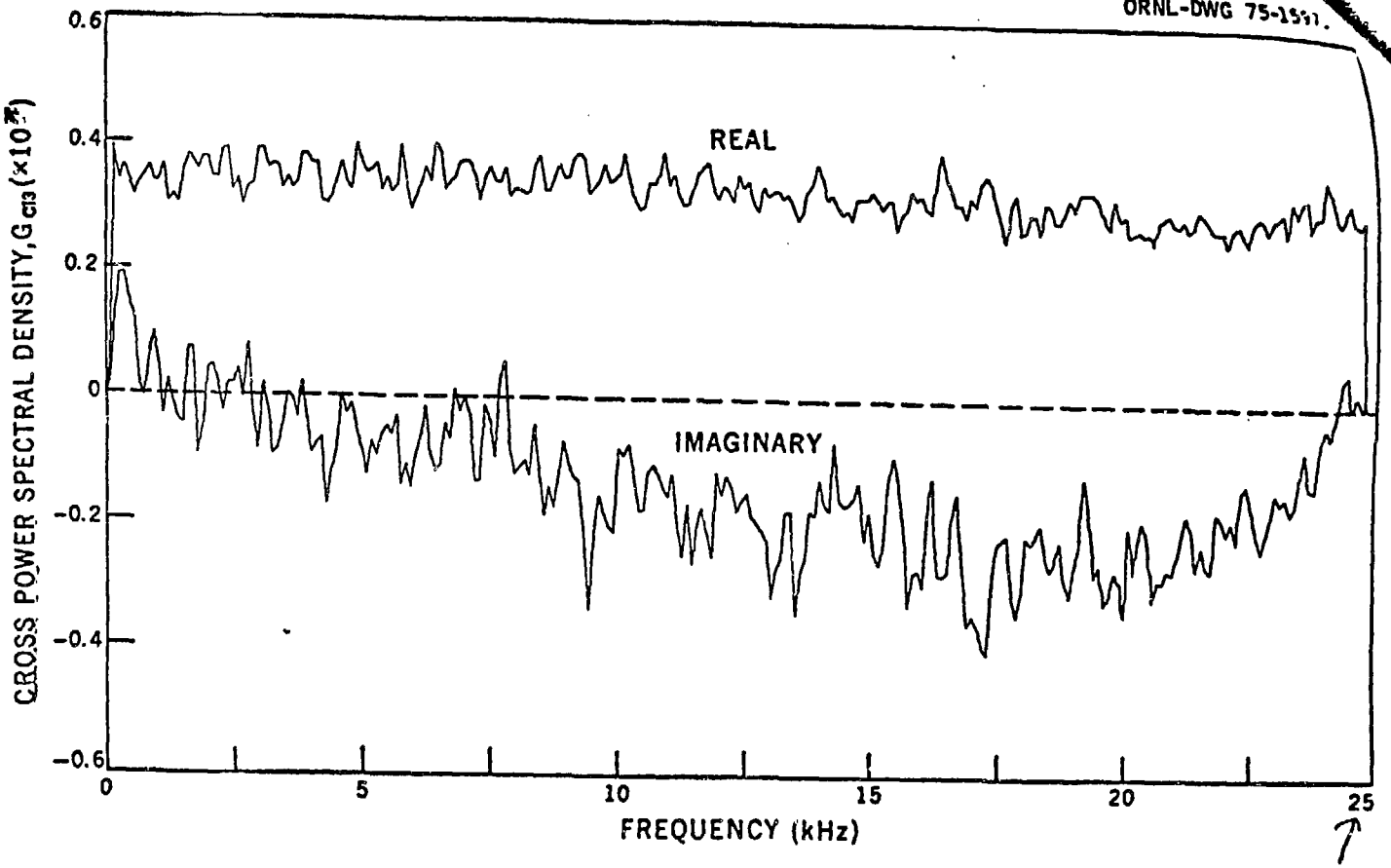
ORNL-DWG 75-19511
REAL
IMAGINARY
CROSS POWER SPECTRAL DENSITY, G_{c13} ($\times 10^{?}$)
0.6
0.4
0.2
0
-0.2
-0.4
-0.6
0
5
10
15
20
25
FREQUENCY (kHz)

F. 2 x 10

? 38

Ratios of Spectral Densities

Various ratios of spectral densities for the measurements with the sphere 29 cent subcritical are plotted in Fig. 11 and were independent of frequency as predicted. The dependence of the ratio of spectral densities $G^{*}_{12}G_{13}/G_{11}G_{23}$ on the ratio of neutrons production rates $F_c I_c \nu_c/(F_i I_i \nu_i + F_c I_c \nu_c)$ was determined by measurements in which the ^{252}Cf chamber was operated in the pulse mode. By raising the discrimination level in this pulse mode detection system, some of the spontaneous fissions of ^{252}Cf were not identified as initiators of fission chains. The rejected events in the ^{252}Cf chamber effectively acted as an inherent source, F_i with the same neutron importance and number of neutrons per fission as neutrons from ^{252}Cf fission. Thus, the ratio of neutron production rates becomes $F_c/(F_c + F_i)$ which equals $F_c(1 - D)/[F_c(1 - D) \quad F_c D]$ or $(1 - D)$ where D is the fraction of the spontaneous fissions of ^{252}Cf that were rejected by the discrimination. The value of D was varied from 0 to 0.8. The results of these measurements for the reactivity of the sphere ~ 29 cents subcritical are given in Fig. 12. As predicted by the theory the ratio of spectral densities varies linearly with the fraction of fission chains initiated by neutrons from californium fission and identified.

If the ratio of spectral densities $G^{*}_{A12}G_{13}/G_{11}G_{23}$ (subscript A signifies frequency response calibration run with a random source) is obtained in the calibration measurements; it can be shown to equal to

$$\frac{1}{B_c(1 + C_\alpha)} \quad \frac{\overline{\nu}_c^2}{\overline{\nu_c^2}}$$

and for pulse mode electronics where all the α decays of ^{252}Cf can be discriminated against, it is equal to $\overline{\nu}_c^2/\overline{\nu_c^2}$ since $B_c(1 + C_\alpha) = 1$. Pulse mode operation of the ^{252}Cf chamber

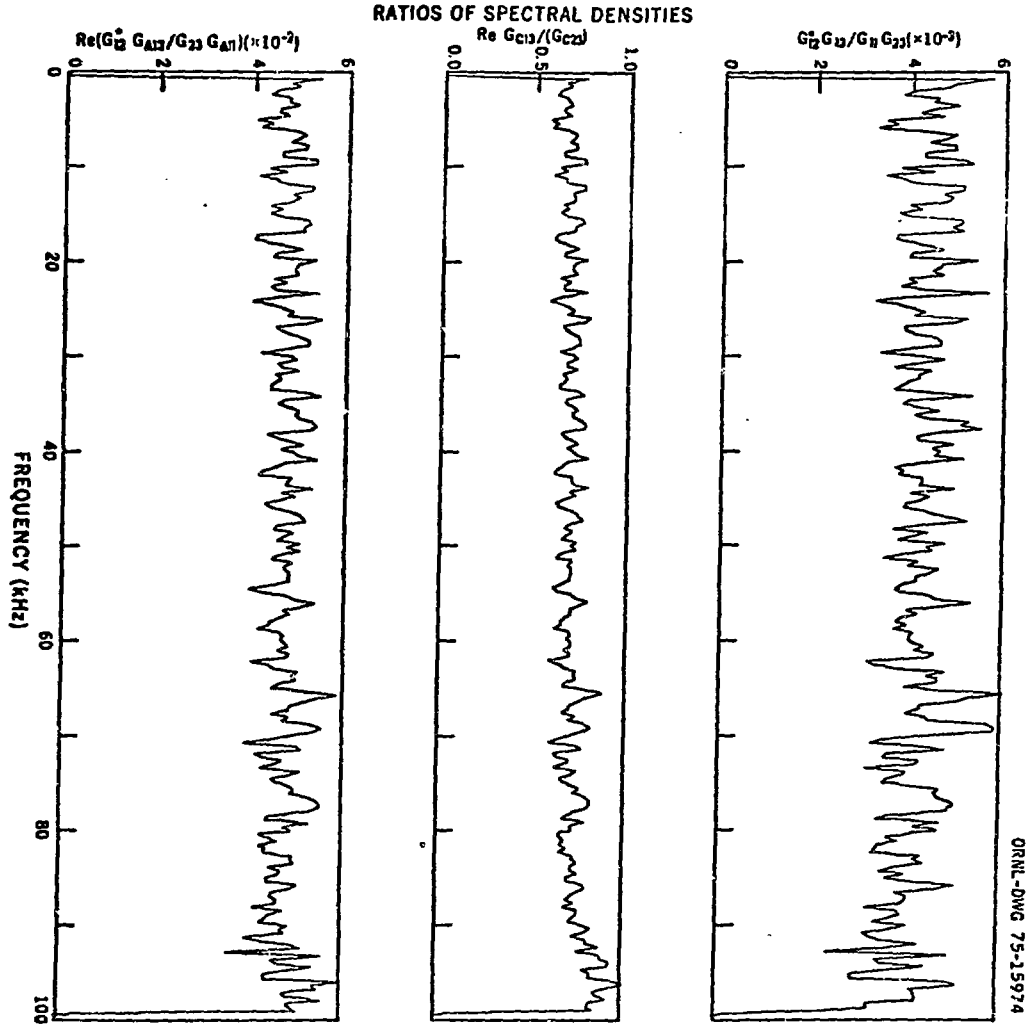
RATIOS OF SPECTRAL DENSITIES
Re(G*12 G213/G23 G211)(×10⁻²)
Re GC13/(GC23)
G*12 G13/G11 G23(×10⁻³)
FREQUENCY (kHz)
0
20
40
60
80
100
0
2
4
6
0.0
0.5
1.0
ORNL-DWG 75-15974

Fig 10 11

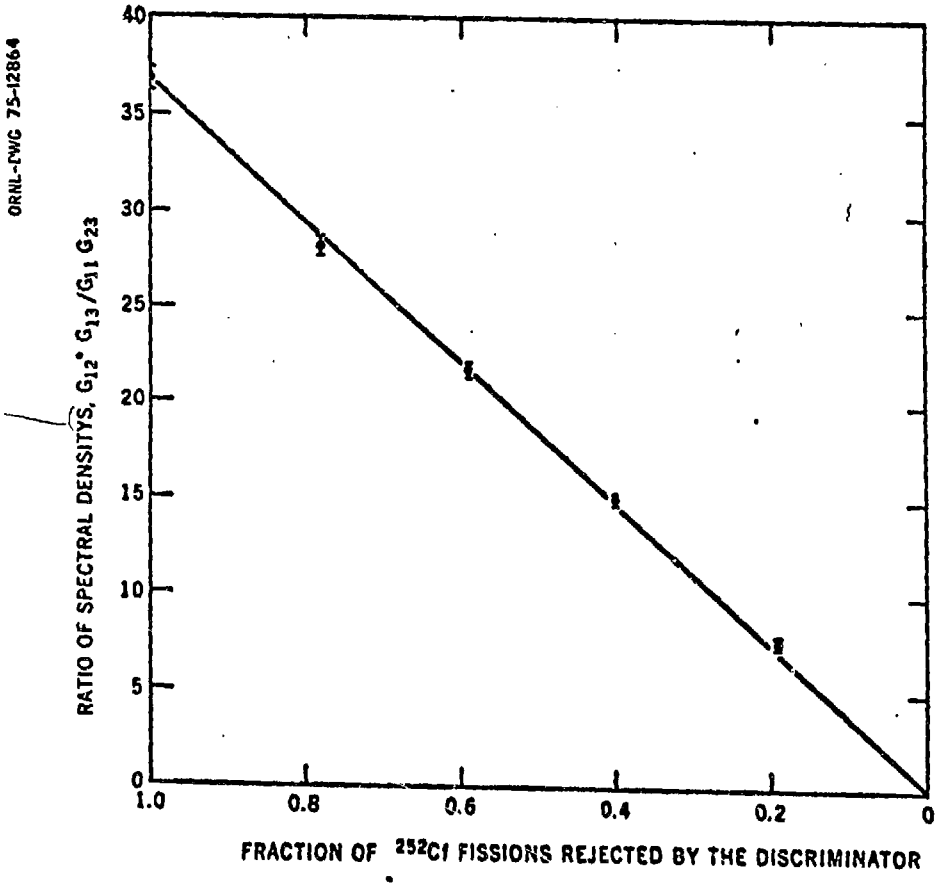

Scale Reversed, 0 should be at left, 1 " " right

the ratio of spectral densities can be used to obtain the value of $\bar{\nu}_c^2/\overline{\nu_c^2}$ which is known from independent direct measurements of the number of neutrons per fission. Good agreement between this determination of $\bar{\nu}_c^2/\overline{\nu_c^2}$ and independent measurements is an excellent way of checking the accuracy and correctness of the Fourier analyzer processing (both hardware and software) system. The value of $\bar{\nu}_c^2/\overline{\nu_c^2}$ obtained from two calibration measurements with the ^{252}Cf chamber operating in the pulse mode are $(0.891 \pm 0.002)^{-1}$ and $(0.905 \pm 0.007)^{-1}$ whereas the value from previous direct measurement of the number of neutrons per fission is $(0.891)^{-1}$ (Ref. 35). This good agreement confirms the correctness of the data accumulation processing and analysis by the total noise analysis system.

Since $\bar{\nu}_c^2/\overline{\nu_c^2}$ is shown very accurately from other measurements, the calibration measurement for the frequency response of the system can be used to determine the values of $B_c(1 + C_\alpha)$. In implementing this method to determine the reactivity in a reactor application the value of $B_c \times (1 + C_\alpha)$ should be determined from the calibration run and this value should be employed in Eq. (15) or (16) to determine the reactivity for the measurements with a reactor.

The independence of the ratio of spectral densities $G_{12}^* G_{13}/G_{11}G_{23}$ of the detection efficiency was verified in measurements in which the detection efficiency was changed in a variety of ways. It was varied in the measurements with the sphere by operating the Li glass scintillator system in both the current and pulse mode resulting in a 62% change in the detection efficiency and the ratio changed only 4%. The detection efficiency was varied by substituting a NaI scintillator (2.54-cm-high, 2.54-cm-diam) for the Li glass scintillator. The NaI was sensitive to gamma rays only while the Li glass was sensitive to both gamma rays and neutrons. Thus not only was the detection efficiency (events/reactor fission) changed, but the type of particles detected. The detection efficiency was also

changed also by moving the Li glass detector from contact with the sphere surface to 4.5 cm away. For all changes the reactivity was reproduced by adding surface mass at adjustment buttons or aluminum reflector until the subcritical power level was the same after the change as before. The results of these measurements showed that, as in the previous experiments with the mock-up of the FFTF, this ratio of spectral densities is independent of detection efficiency.

Reactivity from the Ratio $G_{12}^{*}G_{13}/G_{11}G_{23}$

The reactivity can be obtained from the measurement of the ratio of spectral densities $G_{12}^{*}G_{13}/G_{11}G_{23}$ if the other quantities in Eq. (16) are known. The ratio of fission chains initiated by neutrons from inherent source and ^{252}Cf fission to those initiated by ^{252}Cf fission, Y (Eq. 18) equals unity for these measurements since there is no significant inherent source in the uranium sphere assembly.

The value of P (Eq. 17) for pulse mode operation of the ^{252}Cf chamber simplifies to $RXI\bar{\nu}/I_c\bar{\nu}_c$ since the value of $B_c(1 + C_\alpha)$ equals unity. The average number of prompt neutrons per fission of californium, $\bar{\nu}_c$, used in the interpretation of the measurement, 3.7224 ± 0.0081, is the re-evaluated weighted mean of DeVolpi, (Ref. 36) 3.731 ± 0.008, minus the number of delayed neutrons per fission from Cox, (Ref. 37) 0.0086 ± 0.001. The average number of prompt neutrons per reactor fission, $\bar{\nu}$, was obtained by using the fluxes from transport theory calculations and the ENDF-B-III data to calculate the total number of neutrons per reactor fission which was 2.597. The number of delayed neutrons per reactor fission was obtained with the delayed neutron yields (Ref. 31, 32, 33) and the delayed neutron effectiveness calculations using the forward and adjoint fluxes from S_n transport theory calculations and the delayed neutron spectra of

Batchelor (Ref. 38). The effective delayed neutron fraction calculated in this way is 0.0066. Thus, the number of prompt neutrons per fission is 2.5802.

The importance of the neutrons from the spontaneous fission of californium in the ionization chamber was obtained from previous measurements which compared the source neutrons multiplication of the slightly subcritical sphere with the ^{252}Cf chamber installed with that for the sphere at the same reactivity but with a point source in the center. This measured value is 0.9117 ± 0.0037 (Ref. 29). The average value of the neutron importance was obtained from the measured neutron importance and fission density distribution by averaging the neutron importance over the sphere value using the fission density as a weighting function. The resulting value is 0.5633 ± 0.0003 (Ref. 39).

The value of the Diven factor, $X = \overline{\nu(\nu - 1)}/\bar{\nu}^2$, was obtained by averaging the value of $\nu(\nu - 1)$ and ν over the sphere volume using the fission density obtained from transport theory calculations with the ENDF III-B cross sections as a weighting function. The result obtained, 0.805 is consistent with the previously measured value of Diven.[40]

The value of the factor, R(1.123), which is introduced into the point kinetics equations to account for spatial effects was obtained from measured fission densities and neutron importance distributions.[29] Combining the above quantities using Eq. 10 gives a value of P equal to 0.387.

The expression for P_2 for this assembly in which there is a negligible inherent neutron source reduces to $\overline{\nu_c^2}/\bar{\nu}_c XR$. The value of $\overline{\nu_c^2}$ is obtained from the measurements of Boldeman[35] and is equal to 15.541 ± 0.006. The resulting value of $P_2 = 4.610$.

Using these values and the ratio of spectral densities, the reactivity of the uranium sphere was determined and the results are compared in Table 5 with other measurements.

Table 5. Reactivity determinations from $G^{*}_{12}G_{13}/G_{11}G_{23}$ for the uranium sphere.

Detector	^{252}Cf Chamber	$\frac{G^{*}_{12}G_{13}}{G_{11}G_{23}}$ (X 10^{-4})	Subcritical Reactivity (cents)		
			Other Methods	Noise Analysis	
				Measured Values	Average
LiI	Parallel plate	10.6 ± 0.3 11.9 ± 0.4	7[a]	6.3 ± 0.2 7.0 ± 0.2	6.7 ± 0.2
LiI	Annular	6.9 ± 0.6 6.8 ± 0.3 7.2 ± 0.3 6.6 ± 0.2	8.8[a]	8.5 ± 0.9 8.5 ± 0.4 8.9 ± 0.4 8.2 ± 0.2	8.5 ± 0.3
NaI	Parallel plate	48.2 ± 0.8 46.8 ± 0.8 45.9 ± 0.8 48.2 ± 0.8 48.2 ± 0.8 44.9 ± 0.8	29[b]	28.5 ± 0.5 27.7 ± 0.5 27.2 ± 0.5 28.5 ± 0.5 26.7 ± 0.5 26.6 ± 0.5	27.5 ± 0.8
LiI	Parallel plate	41.6 ± 0.7 41.7 ± 0.8 42.2 ± 0.7 42.7 ± 0.8 42.0 ± 0.7 44.8 ± 0.7 43.2 ± 0.8 42.9 ± 0.7 36.7 ± 0.6 40.6 ± 0.6	29[b]	24.6 ± 0.4 24.7 ± 0.4 24.9 ± 0.4 25.3 ± 0.4 24.9 ± 0.4 26.5 ± 0.4 25.6 ± 0.4 25.6 ± 0.4 21.7 ± 0.4 24.7 ± 0.4	24.7 ± 1.2
LiI	Parallel plate	428 ± 12	230[c]	260 ± 7	260 ± 7
LiI	Parallal plate	410 ± 31	240[c]	249 ± 18	249 ± 18

[a] This value was determined from stable reactor period measurements.

[b] This value was obtained by removal of calibrated surface mass adjustment buttons.

[c] These values were determined by inverse kinetics rod drop measurements in which the lower section of the sphere was displaced slightly from the central section.

The values in the other measurements were determined from stable reactor period measurements, from removal of calibrated surface mass adjustment buttons or by inverse kinetics rod drop measurements in which the lower section was displaced slightly from the central section of the sphere. The values determined are in good agreement with the value from independent measurements, differing between 3 and 15%.

The determination of the reactivity from the ratio of spectral densities Eq. (16) for the cylinders relied on two dimensional calculations for the determination of the following parameter l, l_c, $\bar{\nu}$, X, R. With these calculated parameters, the reactivity was determined and is shown in Fig. 13.

This good agreement confirms the validity of Eq. 6 and verifies for the first time that this method is capable of measuring the reactivity for highly subcritical states. These tests of this method have verified the theory of this measurement method. Thus, a method now exists for reactivity determination which does not require calibration at a known reactivity state, and it can be used in the initial loading of a reactor where subcriticality determination cannot depend on some calibration near delayed criticality and in determining the reactivity of assemblies when sufficient fissionable material to achieve criticality may not be available.

Reactivity Calculations

The ability of Sn transport theory calculations to predict the subcritical reactivity associated with the change in core configuration for fast burst reactors is limited by the ability to accurately mock-up the configuration. Where a configuration change can accurately be represented in the calculation, the reactivity predictions are quite good. The reactivity calculated as a function of cylinder height for 17.77-cm-diam uranium is

Fig 13 Reactivity From: ^{252}Cf Noise Measurements Vs That From Prompt Neutron Decay Constants.

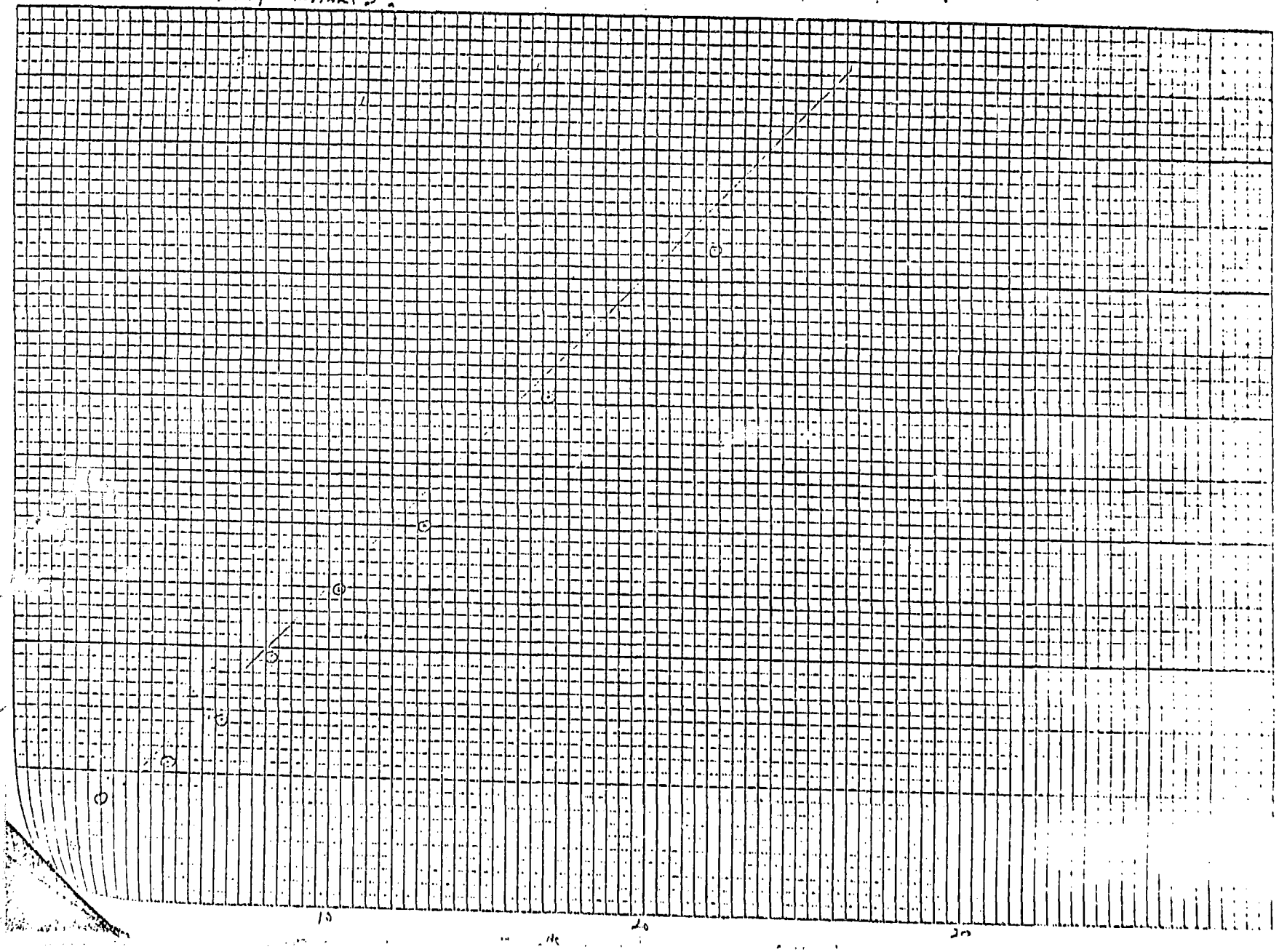

is compared to measurements in Table 6. These two-dimensional calculations used in the Sn transport theory code DOT with ENDF-B-III cross sections. This excellent agreement between measured and calculated reactivities is typical of fast metal systems.

SUMMARY

A variety of methods for reactivity determination have been used satisfactorily for fast metal assemblies. The standard method for reactivity calibration prior to burst initiation and for obtaining the initial reactivity in the excursion is the use of the inhour equations which the validity of point kinetics. The measurement of the stable reactor period during pre-burst calibration and the prompt period during the initial exponential rise of the excursion determines the reactivity. The subcritical reactivities can be determined by the inverse kinetics rod drop method, from prompt neutron decay constant measurements or by methods which utilize the correlation of events in a detector with a source initiating fission chains in the reactor. The IKRD method which requires the reactor be near delayed and the component to be calibrated removed, can be used to obtain control rod calibrations or safety block worths. The prompt neutron decay constant, which can be used to obtain the subcritical reactivity if the value of the prompt neutron decay constant at delayed criticality is known and correction is made for the changes in the prompt neutron lifetime from delayed criticality. The prompt neutron decay constant has been determined by the pulsed neutron method, the Rossi-α method and correlation methods with ^{252}Cf. The latter method will usually be more efficient for data collection for fast metal systems.

The frequency domain methods can be used to obtain the reactivity in the initial loading of a reactor when subcriticality determination methods that depend on calibrations

Table 6. Reactivity for 17.77-cm-diam Uranium Metal Cylinders

Height (cm)	Neutron Multiplication Factor[a]	Reactivity		
		$\frac{\Delta k}{k}$ ($\times 10^{-2}$)	$\frac{\Delta k}{k\beta}$ (dollars)	Measured $\Delta k/k\beta$ (dollars)
12.63	0.9956	0.44	0.67	--
12.22	0.9846	1.56	2.37	2.0
11.59	0.9664	3.48	5.27	5.2
10.80	0.9414	6.22	9.43	9.6
10.18	0.9200	8.71	13.2	13.5
9.23	0.8834	13.20	20.0	20.3
8.28	0.8414	18.81	28.5	28.4

[a] S_n transport theory calculations using ENDF-B III data.

near delayed criticality cannot be used. The latter methods may also be useful in determining the reactivity of assemblies where sufficient material to achieve delayed criticality is not available. These methods using correlations with ^{252}Cf have not been used on fast pulse reactors but have been used successfully on uranium metal systems.

References

1. G. R. Keepin, Physics of Nuclear Kinetics, Addison Wesley, p. 187, 1965.

2. R. E. Peterson and G. A. Newby, Nucl. Sci. Engr. 1, 112-125 (1956).

3. Cesar A. Sastre, Nucl. Sci. Engr. 8, 443 (1960).

4. J. Gengston, Proc. of Second German Conf. 12, 84 (1958).

5. G. DeSaussure, K. Henry, and R. Perez-Belles, Nucl. Sci. Engr. 9, 291 (1961).

6. L. Passel, J. Bengston and D. C. Blair, UCRL-4808 (1957).

7. J. D. Orndoff, Nucl. Sci. Engr. 2, 450-460 (1959).

8. R. W. Badgley and R. E. Uhrig, Nucl. Sci. Engr. 19, 158-163 (1964).

9. C. E. Cohn, Nucl. Sci. Engr. 7, 472-475 (1960).

10. G. M. Hess and R. W. Albrecht, "Polarity Spectral Analysis Reactivity Errors," Trans. Amer. Nucl. Soc. 12, 738 (1969).

11. J. T. Mihalczo and V. K. Paré, "Theory of Correlation Measurements in Time and Frequency Domains with ^{252}Cf," ORNL-TM-4732, Oak Ridge National Laboratory (Nov. 1974).

12. B. J. Toppel, Nucl. Sci. Engr. 5, 88 (1959).

13. J. W. Evans, Los Alamos Report, LA-3045 (1964).

14. J. T. Mihalczo, Nucl. Sci. Engr. 32, 292-301 (1968).

15. J. T. Mihalczo, "Static and Dynamic Measurements with the Assay Pulse Radiation Facility Reactor," ORNL-TM-2330 (June, 1969).

16. R. Gariod, E. Tournier, Vuong Quan Mai, Y P'laige Bilan D'Utilisation Des Reactimetres Dans Les Centrales Nucleaires, IAEA-SM-168/A-11

17. J. B. Bullock, "Reactivity Anomaly Detection in the HFIR with an On-line Computer," Conf. Incipient Failure Diagnosis for Assuring Safety and Availability of Nuclear Power Plants, CONF-671011 (Nov. 1967), p. 61.

18. J. B. Nims, "Malfunction Detection System for Liquid-Metal Fast Breeder Reactors," ibid., p. 211.

19. W. A. Rhoades, F. R. Mynatt, "The DOT-III Two-Dimensional Discrete Ordinates Transport Code," ORNL-TM-4280, Oak Ridge National Laboratory (Sept. 1973).

20. E. E. Gross and J. H. Marable, Nucl. Sci. Engr. 7, 281 (1960).

21. C. A. Preskitt and E. A. Nephen, "Interpretation of Pulsed Source Experiments, Pulsed Neutron Research.," Vol. II, 77-85, IAEA (1965).

22. G. E. Hansen, H. H. Helmick, and J. D. Orndoff, "Neutron Counting Statistics in Basic Fast Critical Assemblies," Proc. Joint Japan United States Seminar on Reactor Noise Analysis (1968).

23. J. T. Mihalczo, Nucl. Sci. Engr. 41, 296 (1970); also, J. T. Mihalczo, "Use of ^{252}Cf as a Randomly Pulsed Neutron Source for Prompt Neutron Decay Measurements," Y-DR-41, UCC-ND Oak Ridge Y-12 Plant (1970).

24. J. T. Mihalczo, Nucl. Sci. Engr. 46, 147-148 (1971).

25. J. T. Mihalczo, Nucl. Sci. Engr. 53, 293-414 (1974).

26. N. G. Sjostrand, Arkiv Fysik 11, 233 (1956).

27. T. Gonzani, Nukleonik 4, 348 (1962).

28. E. Garelis and J. L. Russell, Jr., Nucl. Sci. Engr. 16, 263 (1963).

29. J. T. Mihalczo, Nucl. Sci. Engr. (in press).

30. G. E. Hansen, "Status of Computational and Experimental Correlations for Los Alamos Fast-Neutron Critical Assemblies," Proceedings of Vienna Conference on Fast Reactors, IAEA, paper number 10/53 (1961).

31. G. R. Keepin, T. F. Wimmett, and R. K. Zeigler, Phys. Rev. 107, 1044 (1957).

32. C. F. Masters, M. M. Thorpe, and D. B. Smith, Nucl. Sci. Engr. 36, 202 (1969).

33. M. S. Krick and A. E. Evans, Nucl. Sci. Engr. 47, 311 (1972).

34. G. I. Bell, Nucl. Sci. Engr. 21, 390 (1965).

35. J. W. Boldeman, Nucl. Sci. Engr. 55, 188-202 (1974).

36. A. DeVolpi, "Discrepancies and Possible Adjustments in the 220 m/s Fission Parameters," ANL-7830, Argonne National Laboratory (1971).

37. S. Cox, P. Fields, A. Friedman, R. Sjoblom, and A. Smith, Phys. Rev. 112, 960 (1958).

38. R. Bachelor and H. R. McKhyder, J. Nucl. Energy 3, 7 (1956).

39. J. T. Mihalczo, Nucl. Sci. Engr. 56, 271-290 (1975).

40. B. C. Diven, et.al., Phys. Rev. 101(3), 1012 (1956).